

# ASSESSING SHORELINE EDGE DETECTION FOR THE IMPROVEMENT OF COASTAL IMAGING TECHNIQUES

Siegmund Nuyts, CNRS/GET, Toulouse, France, [siegmund.nuyts@get.omp.eu](mailto:siegmund.nuyts@get.omp.eu)

Eugene Farrell, University of Galway, Ireland, [eugene.farrell@nuigalway.ie](mailto:eugene.farrell@nuigalway.ie)

Sheena Fennell, University of Galway, Ireland, [sheena.fennell@nuigalway.ie](mailto:sheena.fennell@nuigalway.ie)

Stephen Nash, University of Galway, Ireland, [stephen.nash@nuigalway.ie](mailto:stephen.nash@nuigalway.ie)

Remote video imagery using shoreline edge detection is widely used in coastal monitoring in order to acquire measurements of nearshore and swash processes. Some of these systems have very limited flexibility due to their rigid structures and require considerable investment in hardware. As such, there is a need for an autonomous low-cost system ( $\pm\text{€}500$ ) that can be rapidly deployed in the field, while still producing the outcomes required for coastal monitoring. This research presents a sensitivity analysis of time-lapse intervals for two low-cost time-lapse cameras located in a remote coastal area, overlooking a dissipative beach-dune system. Surveyed beach profiles were used to assess changes in beach elevation from December 2021 to February 2022, and a coupled wave-morphology model was developed using SWAN and XBeach to simulate the observed changes.

## INTRODUCTION

Identifying shoreline positions and their shift in response to hydrodynamics is essential to coastal scientists, engineers, and managers (Douglas & Crowell, 2000). With data of where the current shoreline position is, where it has been in the past, as well as being able to predict where it will be in the future, can inform coastal protection strategies. It also provides the ability to calibrate and verify numerical models (Deepika et al., 2014) and assess sea-level change (Leatherman, 2001). Indeed, the detection of shorelines from processed video images is becoming a standard tool in nearshore studies, especially since the commercialization of the ARGUS system (Holman & Stanley, 2007).

Finding a compromise between the optimum sampling rate and the time period over which to average the images remains an ongoing challenge in this research area. Boak and Turner (2005) and Adriolo et al. (2020) found that the sampling interval of 1 Hz over 10 minutes has become a standard procedure but there has been no investigation into the performance of Timex images with different sampling rates. To the best of our knowledge, no analysis has been carried out to investigate the optimum interval of Timex images in coastal research applications.

A low-cost ( $\pm\text{€}500$ ) monitoring system (e.g., off-the-shelf time-lapse cameras) that can be rapidly deployed in the field and/or in remote areas can reduce the initial capital and current investment in monitoring systems and can lead to a fully autonomous system (e.g., no external power source or hardware). The internal batteries from off-the-shelf time-lapse cameras are often small and data is stored on SD cards. This makes them fully autonomous but also reduces the time period that they can sample at field sites.

In addition, there is an urgent need to understand the linkages between coastal shoreline changes and their drivers, in order to better protect coastal communities. The generic controls that influence all coasts include, but are not limited to, wave-wind actions, storm surges, tides, and sediment budget (Devoy, 2015). The magnitude of their respective roles cannot be assessed without the relevant long-term monitoring data on the drivers and responses. Conventional terrestrial and water surveys are not repeated frequently enough for this purpose (Guisado-Pintado & Jackson, 2020) but autonomous monitoring systems and coupled ocean-coastal zone models can provide the long time periods and high temporal resolutions needed.

## AIM AND OBJECTIVES

This research aims to guide the identification of the optimum temporal resolution needed for processing Timex images for shoreline detection. To achieve this, two fully autonomous low-cost time-lapse cameras were deployed in Brandon Bay, Ireland. Timex images were created from high-resolution oblique imagery using different imaging intervals i.e., 1 s, 3 s, 5 s, 10 s, 20 s, and 30 s and shoreline positions were determined from the different Timex images. A sensitivity analysis was then conducted comparing the shoreline positions derived from the different Timex intervals. Furthermore, a coupled wave-morphology modelling system is developed to simulate changes in beach elevation due to storm events.

## METHODOLOGY

Two Brinno TLC2000 time-lapse cameras were installed on the beach (Fig. 1) at elevations of 11 m and 14 m ITM, respectively, and covering alongshore lengths of 200 m and 250 m. The cameras were calibrated using the chessboard approach of Zhang (1999) and the images (Fig. 2) were georectified using ten temporary ground control points at each site.

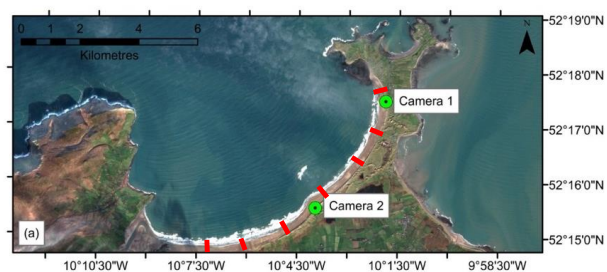


Figure 1 - Brandon Bay study area showing camera locations and survey profile transects



Figure 2 - Sample image from Camera 2

Shoreline edge detection was conducted by detecting the difference between red and blue colour channels (as per Harley et al. (2019)) of time exposure (Timex) images created by taking the average of a number of images taken at regular intervals over 10 minutes. The accuracy of this approach was assessed for images taken at 1 s, 3 s, 5 s, 10 s, 20 s and 30 s (Table 1). A sensitivity analysis was then carried out comparing the shorelines detected for each interval. Wave run-up was determined from Timestack images created by layering together a series of photos taken at timed intervals to generate a single image. Image georectification, and subsequent analyses, were done using MATLAB, with modified versions of the scripts provided by the Coastal Imaging Network (Bruder & Brodie, 2020).

Overview Intervals			
Interval [s]	Time Period [min]	Total Pictures	Memory Demand [MB]
1	10	600	93.3
3	10	200	31.2
5	10	120	18.7
10	10	60	9.5
20	10	30	4.8
30	10	20	3.2

Table 1 - Overview of intervals analyzed in this study

A nested wave model was developed using SWAN comprising (1) a regional northeast Atlantic model with a uniform spatial resolution of  $0.5^\circ$  and time step of 10 minutes and (2) a local Brandon bay model with a uniform spatial resolution of  $0.01^\circ$  and time step of 5 minutes. Wave data from the local model was then used to drive a coastal morphology model developed using XBeach at a spatial resolution of 5 m and time step of 1 minute. The SWAN models were validated against measured wave data for both domains. Wave and beach conditions from December to February 2022 were modelled and compared with surveyed beach profiles measured at seven different transects along the beach (Fig. 1) in December and February 2022.

## RESULTS AND DISCUSSION

All Timex images were processed and the automatically extracted shoreline edges were manually checked in MATLAB, as the image-processing algorithm's performance occasionally produced rogue measurements when precipitation or sea spray affected image quality or during storm/dark conditions when the contrast between sediment and water was too low to distinguish the shoreline edge. Consequently, these Timex images were

excluded from the dataset, resulting in a total of 796 (out of 840) Timex images used in this analysis, from both cameras deployed in Brandon Bay, Ireland.

The RMSE is calculated between the shoreline edges resulting from a 1 s interval and the shoreline edges from the other intervals. The RMSE is defined by the distance between the different transects and consequently, takes into account both x-direction and y-direction of the produced transects. Fig. 3 provides an example of the shoreline edge detected from the MATLAB scripts and the resulting RMSE between two example transects (i.e., 1 s and 5 s). Here, the solid line represents the transect from the 1 s interval and the dashed line the transect from the 5 s interval on 26 February 2022 at high tide. The red shaded area is then the resulting RMSE between the two transects. In this particular example, the x-direction RMSE is 0.368 m, and the y-direction RMSE is 0.321 m.

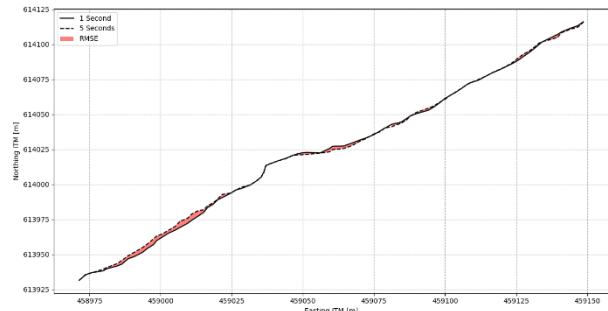


Figure 3 - Example of RMSE between shoreline edge detected on Timex with 1 s interval (solid line) and 5 s interval (dashed line) from 26 February 2022 at high time. The red area represents the RMSE between both lines.

This analysis was carried out for all 796 Timex images and its result is shown in Fig. 4. Here, the overall RMSE ( $RMSE_{mean}$ ) is shown for the shoreline edges derived from the sampling intervals of 3 s (i.e., 200 pictures), 5 s (120 pictures), 10 s (60 pictures), 20 s (30 pictures), and 30 s (20 pictures), compared to an interval of 1 s (600 pictures). The solid line represents  $RMSE_{mean}$  and the shaded area the standard deviation.

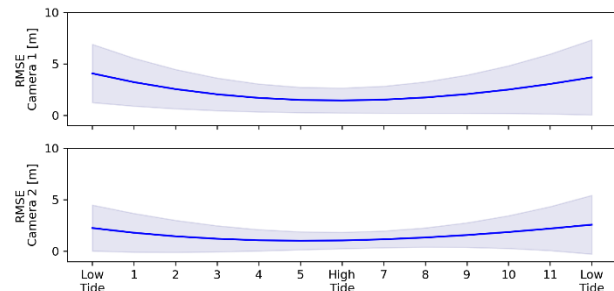


Figure 4 - Mean RMSE (solid blue line) and standard deviation (shaded areas) of all intervals compared to the 1 s interval of the different daylight hours, for (Top) Camera 1; and (Bottom) Camera 2, based on 796 Timex images.

The RMSE and standard deviation are lowest during high tide when the shoreline is closest to the camera position, thus resulting in less distortion and errors. Moreover, the

RMSE for Camera 1 is higher than for Camera 2; this is due to the higher elevation of Camera 2. In general, the higher the camera is positioned above mean sea level (MSL), the greater the FoV (Harley et al., 2019). Indeed, there will be less noise in the shoreline detection due to the greater FoV.

In order to get additional insights into the impact of the image intervals on shoreline accuracy, the RMSE was extracted during high tide for both cameras, as the distortion and errors are the lowest during that time period (Fig. 4). This resulted in 78 shoreline positions (36 for Camera 1 and 42 for Camera 2) for RMSE analysis. Similar to before, the RMSE of shorelines detected using the larger time intervals were calculated relative to those detected from the 1 s interval images; these are shown in Fig. 5.

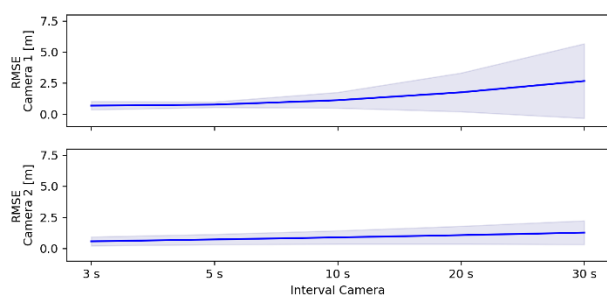


Figure 5 - Mean RMSE (solid blue line) and standard deviation (shaded area), for intervals of 3 s, 5 s, 10 s, 20 s, and 30 s, compared to 1 s interval for (Top) Camera 1; and (Bottom) Camera 2.

## CONCLUSION

The current standard for producing Timex images is averaging 600 pictures over a 10-minute period, with an interval of 1 s. However, there are no studies that investigate the accuracy of shoreline edge detection using Timex images with 1 s interval compared to other intervals. With the focus of deploying a fully autonomous, low-cost time-lapse camera in a remote area, increasing the interval over which Timex images are produced, an increase in interval can increase battery life and reduce memory constraints. As such, shoreline edge detection was carried out in MATLAB from Timex images produced from 1 s, 3 s, 5 s, 10 s, 20 s, and 30 s over a 10-minute period. Consequently, RMSE and standard deviations were calculated between the shoreline edges from a 1 s interval compared to the shoreline edges from the other intervals.

The results of this study showed that there is limited loss of accuracy in shoreline edge detection when increasing the time-lapse interval from 1 s up to 30 s (i.e.,  $RMSE_{max}$  for Camera 1 = 2.8 m and Camera 2 = 1.3 m). In addition, the RMSEs in shoreline edges presented in this study are in a similar range to other studies, highlighting that the presented dataset is of sufficient accuracy to be used for coastal monitoring applications. Moreover, the sensitivity analysis carried out shows that battery life and memory do not necessarily need to be a limiting factor on autonomous operation time, without having an adverse effect on accuracy.

Overall, the analysis of the presented dataset from a low-cost monitoring system showed several advantages over existing techniques reported in similar remotely sensed approaches in coastal monitoring. Firstly, coastal monitoring systems do not necessarily require sophisticated hardware or sophisticated image processing techniques, making their applications easier to replicate. Secondly, the off-the-shelf time-lapse cameras used in this study can be easily and quickly deployed in the field, as well as in remote areas, while still producing outcomes similar to very expensive systems like ARGUS. Thirdly, while elevation above MSL is a limiting factor, this study shows that low elevations can produce meaningful insights into coastal processes. As such, the analysis outlined in this paper results in a better understanding of the setup of coastal imaging systems, which can improve the current methods available for coastal engineers and coastal managers.

## ACKNOWLEDGEMENT

This work was supported by the Geological Survey Ireland Geoscience Research Programme (Grant no. 2020-SC-013) and the EZPONDA project (ERDF ESF 2014-2020).

## REFERENCES

- Andriolo, Mendes, & Taborda. (2020). Breaking Wave Height Estimation from Timex Images: Two Methods for Coastal Video Monitoring Systems. *Remote Sensing*, 12(2).
- Boak & Turner. (2005). Shoreline Definition and Detection: A Review. *Journal of Coastal Research*, 21(4).
- Bruder, & Brodie. (2020). CIRN Quantitative Coastal Imaging Toolbox. SOFTWAREX, 12.
- Deepika, Avinash, & Jayappa. (2014). Shoreline change rate estimation and its forecast: remote sensing, geographical information system and statistics-based approach. *International Journal of Environmental Science and Technology*, 11(2).
- Devoy. (2015). The Development and Management of the Dingle Bay Spit-Barriers of Southwest Ireland. *Coastal Spits*.
- Douglas & Crowell. (2000). Long-Term Shoreline Position Prediction and Error Propagation. *Journal of Coastal Research*, 16(1).
- Guisado-Pintado & Jackson. (2020). Monitoring Cross-shore Intertidal Beach Dynamics using Oblique Time-lapse Photography. *Journal of Coastal Research*, 95(SI).
- Harley, Kinsela, Sánchez-García, & Vos. (2019). Shoreline change mapping using crowd-sourced smartphone images. *Coastal Engineering*, 150.
- Holman & Stanley. (2007). The history and technical capabilities of Argus. *Coastal Engineering*, 54(6).
- Leatherman. (2001). Chapter 8 Social and economic costs of sea level rise. *International Geophysics*, 75.
- Zhang, Z. (1999). Flexible camera calibration by viewing a plane from unknown orientations. *Seventh IEEE International Conference on Computer Vision*.